THE IMPORTANCE OF PHOTODISSOCIATIVE TRICHLOROMETHANOL FOR ATMOSPHERIC CHEMISTRY

Max MÜHLHÄUSER[a,b],*, Melanie SCHNELL[a,c] and Sigrid D. PEYERIMHOFF[a1]

 [a] *Institut für Physikalische und Theoretische Chemie, Universität Bonn, Wegelerstrasse 12, 53115 Bonn, Germany; e-mail: [1] unt000@uni-bonn.de*

 [b] *Verfahrens- und Umwelttechnik (FH), Management Center Innsbruck, Egger-Lienz-Strasse 120, A-6020 Innsbruck, Austria; e-mail: max.muehlhaeuser@mci.edu*

 [c] *Institut für Physikalische Chemie, Universität Hannover, Callinstrasse 3-3A, 30167 Hannover, Germany; e-mail: melanie.schnell@pci.uni-hannover.de*

Dedicated to Professor Rudolf Zahradník on the occasion of his 75th birthday.

Multireference configuration interaction calculations are carried out for ground and excited states of trichloromethanol to investigate two important photofragmentation processes relevant to atmospheric chemistry. For CCl_3OH five low-lying excited states in the energy range between 6.1 and 7.1 eV are found to be highly repulsive for C–Cl elongation leading to Cl_2COH (X^2A') and Cl (X^2P). Photodissociation along C–O cleavage resulting in Cl_3C (X^2A') and OH ($X^2\Pi$) has to overcome a barrier of about 0.8 eV ($1^3A''$, $1^1A''$) and 1.2 eV ($1^3A'$) because the low-lying excited states $1^1A''$, $1^3A'$ and $1^3A''$ become repulsive only after elongating the C–O bond by about 0.3 Å.

Keywords: Multireference configuration interaction; DFT; *Ab initio* calculations; Photolysis; Chlorinated alcohols; Radicals; Photodissociation.

It is well known that the destruction of ozone in the stratosphere is accelerated by a system of reaction cycles involving active chlorine species like Cl and ClO radicals[1-3]. Therefore detailed knowledge of the atmospheric chemistry of halogen-containing compounds is of great importance for understanding the destruction of the Earth's protecting ozone layer in the stratosphere. Especially there is a great interest in species which can act as chlorine reservoirs like the chlorinated methanol derivatives $CH_{2-x}Cl_{1+x}OH$ (x = 1, 2)[4-9]. As a consequence, the formation of these species can lead to a deceleration of the destruction of the ozone layer.

Recently Bozzelli *et al.* published a theoretical study of equilibrium structures and thermochemical properties of several chloromethanol derivatives[10]. For monochloromethanol CH_2ClOH, they calculated an enthalpy of formation ΔH_{f298}^0 of –58.07 kcal/mol. For dichloromethanol $CHCl_2OH$ and

trichloromethanol CCl_3OH, they obtained an about 8 kcal/mol lower ΔH^0_{f298} value than for CH_2ClOH.

The photochemistry of these chlorinated methanol derivatives is very important for the description of the atomic chlorine cycle in atmospheric chemistry since the formation of these derivatives during polar night leads to a deceleration of the ozone degradation whereas chlorine re-liberation *via* photofragmentation is very probable. In earlier studies we already examined excited states and photodissociative bond cleavage of monochloromethanol CH_2ClOH [11,12] and dichloromethanol $CHCl_2OH$ [13–15] to investigate their relevance as chlorine reservoirs in atmospheric chemistry. We found that the C–O cleavage has to overcome a barrier of about 0.3 eV for CH_2ClOH [12] and of about 0.5 eV for $CHCl_2OH$ [15]. On the other hand, for photofragmentation *via* C–Cl cleavage we calculated five low-lying excited states to be highly repulsive for both CH_2ClOH and $CHCl_2OH$ [12,15].

In continuation of this prior work the present study investigates trichloromethanol CCl_3OH and its influence on the atomic chlorine cycle. The compound is also very important since it has the threefold number of chlorine atoms and its stability is comparable with that of $CHCl_2OH$. Therefore we perform large-scale multireference configuration interaction (MRD-CI) calculations of its excited states and its photofragmentation along the C–Cl and C–O cleavage.

COMPUTATIONAL TECHNIQUES

The equilibrium geometries of trichloromethanol CCl_3OH and the dichloro(hydroxy)methyl radical Cl_2COH were adopted from recent work of Bozzelli *et al.*[10] They optimized these structures at the B3LYP/6-31G** level. For comparison, we optimized the equilibrium geometries of the other fragments, the trichloromethyl radical Cl_3C and the hydroxyl radical OH, using the same method and basis set employing the GAUSSIAN 98 program package[16]. The relative stabilities of the various species considered were also computed at the coupled cluster level CCSD including singles and doubles. In addition, we employed some more extensive multireference CI calculations. Zero-point corrections have been estimated from our DFT calculations.

For the computations of excited states, we used a correlation consistent AO basis set of triple zeta quality cc-p-VTZ+sp [17] augmented by two d- and one f-polarization functions for carbon, oxygen and chlorine. The exponents taken are $\alpha_d(C) = 1.09, 0.31$, $\alpha_d(O) = 2.314, 0.645$, $\alpha_d(Cl) = 1.046, 0.344$, $\alpha_f(C) = 0.76$, $\alpha_f(O) = 1.428$ and $\alpha_f(Cl) = 0.706$. In addition, this basis

set was enlarged by s-Rydberg functions located at the carbon and a negative ion function for the chlorine centers. The exponents taken are $\alpha_r(C)$ = 0.023 for the s-Rydberg function and $\alpha_r(Cl)$ = 0.049 for the negative ion function at the chlorine. On the other hand, prior calculations on similar chlorinated methanol derivatives like chloromethanol CH_2ClOH [11,12] and dichloromethanol $CHCl_2OH$ [13–15] employing a smaller polarized cc-p-VDZ+sp basis set of double zeta quality[17] with the exponents $\alpha_d(C)$ = 0.55, $\alpha_d(O)$ = 1.185, $\alpha_d(Cl)$ = 0.60 and the same exponents for the s-Rydberg function at the carbon and the negative ion function for the chlorine site show almost no changes in excitation energies and transition probabilities of the excited states examined. The values obtained are in reasonable agreement with the results of the more extensive computations[6,11–15]. Therefore, this more economic cc-p-VDZ+sp basis has been used for the computations of the numerous points of the potential energy curves presently examined similar to our earlier work.

The computations of the electronically excited states were performed with the selecting multireference single and double excitation configuration interaction method MRD-CI implemented in the DIESEL program package[18]. The selection of reference configurations can be carried out automatically in dependence on a chosen summation threshold (here 0.85), which means that the sum of the squared coefficients of all reference configurations selected for each state (root) is above this given threshold of 0.85. From this selected set of reference configurations (mains), all single and double excitations in the form of configuration state functions (CSFs) are generated. From this set all configurations with an energy contribution $\Delta E(T)$ above a given threshold T were selected, *i.e.* the contribution of a configuration larger than this value relative to the energy of the reference set is included in the final wavefunction. A selection threshold of $T = 10^{-7}\ E_h$ was used for both isomers. The effect of those configurations which contribute less than $T = 10^{-7}\ E_h$ is accounted for in the energy computation (E(MRD-CI)) by a perturbative technique[19,20]. The contribution of higher excitations is estimated by applying a generalized Langhoff–Davidson correction formula $E(\text{MRD-CI+Q}) = E(\text{MRD-CI}) + (1 - c_0^2)\ [E(\text{ref}) - E(\text{MRD-CI})]/c_0^2$, where c_0^2 is the sum of squared coefficients of the reference species in the total CI wavefunction and E(ref) is the energy of the reference configurations.

We examined the lowest six excited states (three singlet and three triplet states) for C–O cleavage and the lowest eight states (four singlet and four triplet states) for photofragmentation *via* C–Cl cleavage. The set of reference configurations per irreducible representation (IRREP) was in the range

between 9 and 14 for CCl_3OH. An analysis of the molecular orbitals (MO) involved in these selected reference configurations justified the prior choice of treating 32 electrons as active while keeping the remaining electrons in doubly-occupied orbitals (frozen). The number of configuration state functions (CSFs) directly included in the energy calculations is as large as 2.4 million (singlet) and 3.3 million (triplet) for CCl_3OH selected from a total space of 4.8 million (singlet) and 5.6 million (triplet) generated configurations using the cc-p-VDZ+sp basis set. Employing the cc-p-VTZ+sp basis set, the number of CSFs directly included in the energy calculations are as large as 3.1 (singlet) selected from a total space of 5.2 (singlet) generated configurations.

RESULTS AND DISCUSSION

For the photofragmentation of trichloromethanol CCl_3OH we examined two possible pathways. One was to elongate the C–O bond stepwise in the range between the equilibrium bond length of 1.351 and 10 Å according to the reaction

$$CCl_3OH \rightarrow Cl_3C + OH \ , \qquad (1)$$

while all other geometry parameters were optimized using the density functional method with the B3LYP functional as implemented in the Gaussian 98 program package[16]. It is well known that reliable equilibrium structures are obtained using this B3LYP functional. In addition, we have explicitly shown in a recent paper[11] that a reasonable equilibrium geometry of the monochlorinated CH_2ClOH is already obtained at the B3LYP/6-31G* level of theory.

As a second model we considered a photofragmentation along the C–Cl cleavage according to the reaction

$$CCl_3OH \rightarrow Cl_2COH + Cl \qquad (2)$$

by elongating one C–Cl bond stepwise from the equilibrium length of 1.782 to 10 Å. Again all other geometry parameters are optimized.

In Table I we summarize the fragmentation energies we calculated for the reactions (1) and (2). The values obtained at the different theoretical levels (B3LYP, CCSD and MRD-CI(+Q)) are in reasonable agreement with each other. For C–O cleavage (1), we computed a fragmentation energy ΔE(MRD-CI+Q) of 87.7 kcal/mol. Inclusion of zero-point corrections reduces this value to 83 kcal/mol. For C–Cl cleavage, we obtained a fragmentation

energy of ΔE(MRD-CI+Q +ΔZPE) = 76.6 kcal/mol including zero-point corrections. This value is in reasonable agreement with Bozzelli *et al.*[10], who calculated a fragmentation energy for C–Cl cleavage of 72.34 kcal/mol at the B3LYP/6-31G** level (at 298 K). A simultaneous elongation of two C–Cl bonds leading to *trans*-Cl–C–OH and two separated chlorine atoms

$$CCl_3OH \rightarrow ClCOH + 2\ Cl \tag{3}$$

is energetically not favoured. We obtained a fragmentation energy of ΔE(MRD-CI+Q) = 120 kcal/mol which is significantly higher than that calculated for the two other pathways investigated.

It can be seen from Fig. 1 that following pathway (*1*) (C–O cleavage), the C–Cl bond lengths in Cl_3C are somewhat shortened in line with the expected increased double bond character for an sp^2 carbon center in Cl_3C compared to an sp^3 carbon center in CCl_3OH. In addition, for C–Cl cleavage, the remaining C–Cl and C–O bonds are also somewhat shortened in the Cl_2COH radical again in line with the increased double bond character for C–Cl and C–O. Generally, the equilibrium geometries of the photofragments are obtained in reasonable agreement with what is known from the literature. For example the experimental OH ($^2\Pi$) distance is 0.96966 Å (ref.[21]) compared to our calculated value of 0.971 Å.

TABLE I
Fragmentation energies ΔE (kcal/mol) of trichloromethanol CCl_3OH at different levels of theoretical treatment (B3LYP, CCSD, MRD-CI) as explained in the text, not accounting for zero-point energies ZPE. The values have been obtained with the cc-p-VTZ basis set at the B3LYP/6-31G**-optimized geometries. Relative stabilities as obtained in a multireference single- and double-excitation configuration interaction (MRD-CI) including the Davidson correction (MRD-CI+Q) are also given. $E(T)$ is the energy at a threshold ($T = 10^{-7}\ E_h$) as explained in the computational techniques

Fragmentation channel	Cl_2COH (X^2A') + Cl (X^2P)	Cl_3C (X^2A') + OH ($X^2\Pi$)
ΔE(B3LYP)	75.5	92.9
ΔZPE^a	–1.6	–4.7
ΔE(CCSD)^b	72.5	87.8
$\Delta E(T)$	74.3	83.9
ΔE(MRD-CI)	70.5	85.1
ΔE(MRD-CI+Q)	78.2	87.7

^{a} Zero-point corrections have been estimated from the B3LYP/6-31G** calculations. ^{b} cc-p-VDZ basis set.

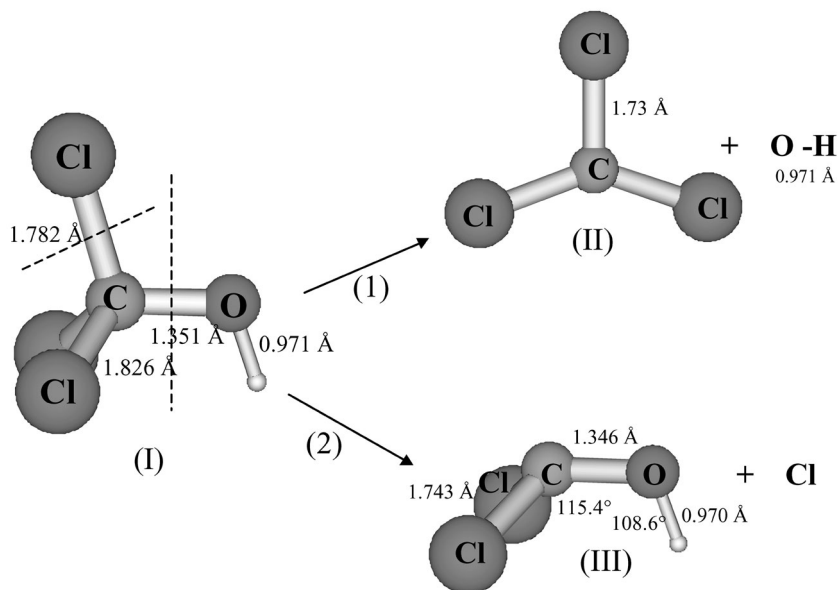FIG. 1
Equilibrium geometries of trichloromethanol CCl$_3$OH (I) adopted from ref.[10] and its possible photofragments obtained from our B3LYP/6-31G** optimization as explained in the text. The dissociation processes studied correspond to the C–Cl (*2*) and C–O (*1*) cleavage
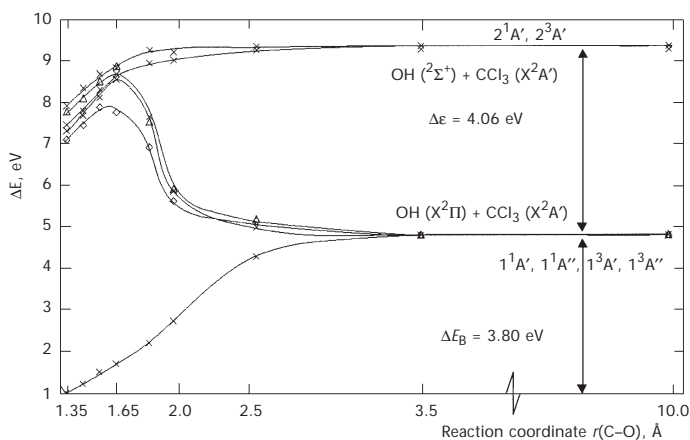

FIG. 2
DIESEL-MRD-CI potential energy curves of the lowest six states of trichloromethanol CCl$_3$OH along a C_s symmetric fragmentation pathway breaking the C–O bond. The fragmentation energy ΔE_B and the energy difference $\Delta \varepsilon$ between the two dissociation channels are illustrated

The potential energy curves for the two pathways investigated are presented in Figs 2 and 3. It can be seen from these figures in conjunction with Table I that the formation of trichloromethanol CCl_3OH in its ground state from the fragments Cl_2COH and Cl as well as from Cl_3C and OH is energetically favoured. Both cuts through the ground state potential energy surfaces are computed to be barrier-free. On the other hand, fragmentation processes according to (*1*) and (*2*) require more than 75 kcal/mol on the ground state surface and are, consequently, very unlikely.

In Table II, we present for completeness the electronic absorption spectrum of trichloromethanol up to 8.5 eV. The comparison between the cc-p-VTZ+sp basis set and the more economic cc-p-VDZ+sp basis shows only minor changes for the excitation energies and transition probabilities. The ground state configuration of singlet CCl_3OH is $(10a')^2 (6a'')^2$. Due to spin conservation, transitions to excited singlet states are most likely. But recent experimental studies have shown that spin-orbit coupling is non-negligible for some chlorine species like HOCl [6,22,23]. Consequently, transitions to excited triplet states of CCl_3OH are also considered in the present study.

In Fig. 2 the calculated potential energy curves for the lowest six states for C–O cleavage (*1*) are given. It is seen that the first excited states have to overcome barriers when elongating the C–O bond. These barriers are of
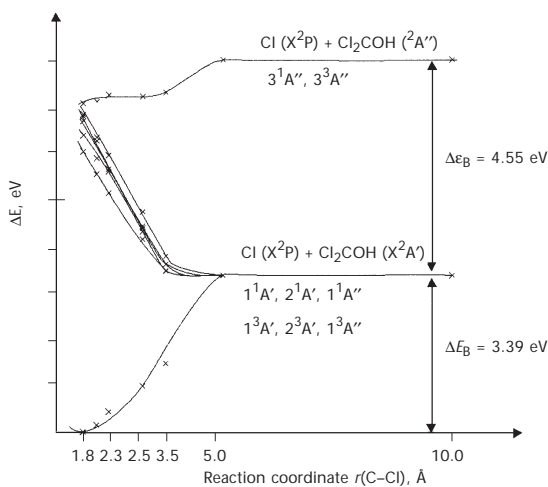

F_IG_. 3
DIESEL-MRD-CI potential energy curves of the lowest eight states of trichloromethanol CCl_3OH along the C–Cl cleavage. The fragmentation energy ΔE_B and the energy difference $\Delta \varepsilon$ between the two dissociation channels are illustrated

the order of 0.79 eV for the $1^3A''$ state, of 0.72 eV for the $1^1A''$ state and of 1.22 eV for the $1^3A'$ state. Consequently, photofragmentation breaking the C–O bond is hindered by these barriers. If the equilibrium bond distance is elongated by about 0.3 Å or more, the three excited states $1^3A''$, $1^3A'$ and $1^1A''$ become repulsive. Together with the ground state, they correlate with the first dissociation channel at 3.80 eV (87.7 kcal/mol) which corresponds to the ground states of Cl_3C (X^2A') and OH ($X^2\Pi$). The repulsive behaviour of these states after elongating the C–O bond can be understood from qualitative MO considerations. Contour diagrams of some important occupied and virtual MOs are shown in Fig. 4. All three states are populated by excitations into the LUMO 11a' which shows mainly the σ^*(C–Cl)-type character. Besides this, it also possesses C–O nonbonding contributions.

The second dissociation channel corresponds to OH in its excited $^2\Sigma^+$ state. The calculated energy difference $\Delta\varepsilon$ of 4.06 eV is in good agreement with the 4.05 eV reported in the literature[21] for the $^2\Sigma^+ \leftarrow {}^2\Pi$-transition.

TABLE II
Calculated vertical electronic transition energies ΔE (eV) and oscillator strengths f from the ground state configuration $(10a')^2 (6a'')^2$ of trichloromethanol CCl_3OH to its low-lying electronic states and comparison between the cc-p-VDZ+sp and cc-p-VTZ+sp basis sets as explained in the text. The values have been obtained at the MRD-CI+Q-level as explained in the computational techniques

State	Excitation	ΔE^a	f^a	ΔE^b	f^b
X^1A'	$(10a')^2(6a'')^2$	0.0	–	0.0	–
$1^3A''$	$6a'' \rightarrow 11a'$	6.09	–		
$2^3A''$	$5a'' \rightarrow 11a'$	6.31	–		
$1^3A'$	$10a' \rightarrow 11a'$	6.45	–		
$1^1A''$	$6a'' \rightarrow 11a'$	6.77	0.010	6.77	0.005
$3^3A''$	$4a'' \rightarrow 11a'$	6.87	–		
$2^3A'$	$9a' \rightarrow 11a'$	6.91	–		
$2^1A''$	$5a'' \rightarrow 11a'$	7.07	0.013	6.90	0.01
$3^3A'$	$8a' \rightarrow 12a'$	7.13	–		
$2^1A'$	$10a' \rightarrow 11a'$	7.15	0.044	7.21	0.052
$3^1A'$	$9a' \rightarrow 11a'$	7.71	0.020	7.78	0.084
$4^1A'$	$8a' \rightarrow 11a'$	7.87	0.002		
$3^1A''$	$4a'' \rightarrow 11a'$	7.99	0.145		
$4^1A''$	$3a'' \rightarrow 11a'$	8.54	0.011		

[a] cc-p-VDZ+sp basis set. [b] cc-p-VTZ+sp basis set.

The upper states $2^3A'$ and $2^1A'$ in Fig. 2 are not repulsive and thus fragmentation into Cl_3C and OH in its excited $^2\Sigma^+$ state is unlikely and therefore less important.

As can be seen from Fig. 3, we have calculated the potential energy curves for the lowest eight states for C–Cl cleavage (*2*) (four singlet and four triplet states). We found five highly repulsive excited states $1^1A''$, $2^1A'$, $1^3A''$, $1^3A'$ and $2^3A'$ leading to the first dissociation channel Cl_2COH (X^2A') and Cl (X^2P) at 3.39 eV (78.2 kcal/mol). The repulsive character of these five excited states can again be understood from qualitative MO considerations (Fig. 4). The LUMO 11a′ is populated in all these states and it is highly σ^*(C–Cl)-antibonding. It is populated in the $1^3A''$ and $1^1A''$ states by 6a″ → 11a′ excitation (HOMO-LUMO) and in the states $1^3A'$ and $2^1A'$ by 10a′ → 11a′ excitation. The repulsive $2^3A'$ state results from a transition 9a′ → 11a′ as can be seen from Table II.

The second dissociation channel corresponds to the first excited state of Cl_2COH ($^2A''$). It is calculated at 7.94 eV, the energy difference between both dissociation channels $\Delta\varepsilon$ is calculated with 4.55 eV. The excited states
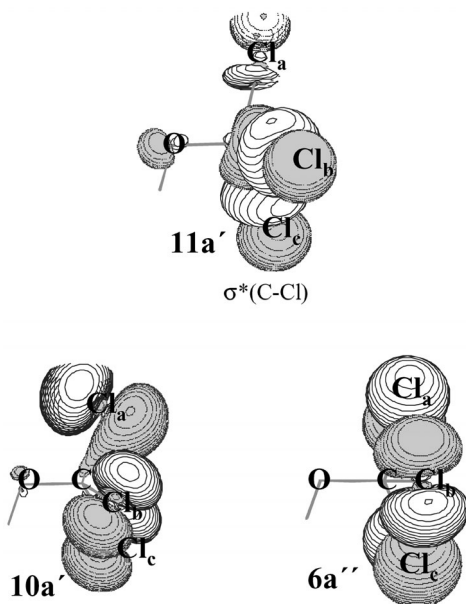

Fig. 4

Charge density contours of characteristic occupied valence orbitals (6a″, 10a′) and the lowest virtual molecular orbital LUMO (11a′) of CCl_3OH

leading to this second dissociation channel are found to be not repulsive and, consequently, the fragmentation of CCl_3OH into Cl and Cl_2COH in its first excited state $^2A''$ is less important.

The fragmentation energies for C–O cleavage for all three investigated $CH_{2-x}Cl_{1+x}OH$ ($x = 1, 2$) species[12,15] are of the same order of magnitude (Table III). For CH_2ClOH we calculated ΔE(MRD-CI+Q+ΔZPE) = 88.2 kcal/mol [12], for $CHCl_2OH$ we found a value of ΔE(MRD-CI+Q+ΔZPE) = 87.8 kcal/mol [15] and for CCl_3OH the calculated fragmentation energy is ΔE(MRD-CI+Q+ΔZPE) = 83 kcal/mol. On the other hand, we found energy barriers for the first excited states of the three species. The barrier height for CH_2ClOH is about 0.3 eV for the first three excited states $1^1A''$, $1^3A'$ and $1^3A''$ (ref.[12]). For $CHCl_2OH$ we found barriers of about 0.5 eV [15] while for CCl_3OH the barrier heights are in the range 0.8–1.2 eV.

For C–Cl cleavage the fragmentation energies are again of the same order of magnitude. We calculated ΔE(MRD-CI+Q+ΔZPE) = 82.3 kcal/mol for CH_2ClOH [12], ΔE(MRD-CI+Q+ΔZPE) = 74.3 kcal/mol for $CHCl_2OH$ [15] and ΔE(MRD-CI+Q+ΔZPE) = 76.6 kcal/mol for CCl_3OH (Table III). As already discussed above and in our prior studies of CH_2ClOH and $CHCl_2OH$ [12,15], we found five highly repulsive excited states for C–Cl cleavage for all three investigated species. In addition, we found that the first transition $1^3A'' \leftarrow X^1A'$ is lowered systematically with the amount of chlorine atoms (CH_2ClOH:

TABLE III
Fragmentation energies ΔE (kcal/mol) of monochloromethanol CH_2ClOH and dichloromethanol $CHCl_2OH$ at different levels of theoretical treatment (B3LYP, CCSD(T), MRD-CI) as explained in the text, not accounting for zero-point energies ZPE. The values have been obtained with the cc-p-VTZ basis set at the B3LYP/6-31G**-optimized geometries. Relative stabilities obtained on the $E(T)$ (threshold $T = 10^{-7}$ E_h), MRD-CI and MRD-CI+Q level as explained in the computational techniques are also given

Fragmentation channel	CH_2OH (X^2A'') + Cl (X^2P)	$ClCH_2$ (X^2B_2) + OH($X^2\Pi$)	$ClCHOH$ (X^2A) + Cl (X^2P)	Cl_2CH (X^2A') + OH ($X^2\Pi$)
ΔE(B3LYP)	81.7	98.3	74.1	97.5
ΔZPE	–3.8	–8.1	–2.51	–5.64
ΔE(CCSD(T))	80.9	96.0	73.7^a	95.7^a
$\Delta E(T)$	89.1	98.0	73.5	91.1
ΔE(MRD-CI)	88.3	97.3	74.9	91.4
ΔE(MRD-CI+Q)	86.1	96.3	76.8	93.4

^{a} cc-p-VDZ basis set.

6.86 eV, CHCl$_2$OH: 6.46 eV and CCl$_3$OH: 6.09 eV)[12,15]. This lowering is in line with the smaller HOMO-LUMO gap of trichloromethanol.

CONCLUSIONS

Large-scale *ab initio* multireference configuration interaction (MRD-CI) calculations are employed to investigate possible photofragmentation of trichloromethanol CCl$_3$OH along C–O (*1*) and C–Cl cleavage (*2*). A simultaneous elongation breaking two C–Cl bonds (*3*) is energetically not favoured. On the ground state surface, dissociations along (*1*) and (*2*) are not very likely; on the other hand, formation of trichloromethanol according to the reverse reactions (*1*) and (*2*) is possible in the ground states and these formation processes are calculated to be barrier-free. The fragmentation energies for (*1*), (*2*) and (*3*) obtained at the different levels of theory (B3LYP/cc-p-VTZ, CCSD/cc-p-VDZ, MRD-CI+Q/cc-p-VTZ+sp) are in reasonable agreement with each other and the values deduced from the work of Bozzelli *et al.*[10]. CCl$_3$OH is stabilized relative to its products of (*1*) by about 83 kcal/mol and of (*2*) by about 76.6 kcal/mol (ΔE(MRD-CI+Q+ΔZPE)).

Photodissociation breaking the C–O bond has to overcome a barrier of about 0.8 eV ($1^3A''$, $1^1A''$) and about 1.2 eV ($1^3A'$) because these excited states become repulsive only if the equilibrium C–O distance is elongated by about 0.3 Å.

Five low-lying excited states (three triplets and two singlets) with vertical excitation energies between 6.1 and 7.1 eV are found to be highly repulsive for C–Cl elongation leading to the dissociation channel Cl$_2$COH (X^2A') and Cl (X^2P). The repulsive character of these states can be understood on the basis of qualitative MO considerations: The lowest virtual molecular orbital (LUMO) 11a′ is of antibonding σ^*(C–Cl) character and, therefore, photofragmentation breaking the C–Cl bond involving excited states, in which this repulsive σ^*(C–Cl)-type LUMO 11a′ is populated, is very likely.

The computed energy for the first transition ($1^3A'' \leftarrow X^1A'$) is lowered from 6.86 eV (CH$_2$ClOH) to 6.46 eV (CHCl$_2$OH) to 6.09 eV in CCl$_3$OH. Thus chlorine re-liberation is easiest for CCl$_3$OH whereas monochloromethanol CH$_2$ClOH is considered to be the most stable chlorine reservoir.

REFERENCES

1. Farman J. C., Gardiner B. G., Shanklin J. D.: *Nature* **1985**, *315*, 207.
2. Anderson J. G., Toohey D. W., Brune W. H.: *Science* **1991**, *251*, 39.
3. Solomon S.: *Nature* **1990**, *347*, 347.
4. a) Crutzen P. J., Müller R., Brühl C., Peter T.: *Geophys. Res. Lett.* **1992**, *19*, 11; b) Crutzen P. J., Müller R., Brühl C., Peter T.: *Geophys. Res. Lett.* **1992**, *19*, 1113.
5. Helleis F., Crowley J. N., Moortgat G. K.: *Geophys. Res. Lett.* **1994**, *21*, 1795.
6. Li Y., Francisco J. S.: *J. Chem. Phys.* **1999**, *111*, 8384.
7. Jungkamp T. P. W., Kirchner U., Schmidt M., Schindler R. N.: *J. Photochem. Photobiol., A* **1995**, *91*, 1.
8. Schindler R. N., Liesner M., Schmidt S., Kirchner U., Benther Th.: *J. Photochem. Photobiol., A* **1997**, *107*, 9.
9. Crowley J. N., Helleis F., Müller R., Moortgat G. K., Crutzen P. J.: *J. Geophys. Res.* **1994**, *99*, 20683.
10. Sun H., Bozzelli J. W.: *J. Phys. Chem.* **2001**, *105*, 4504.
11. Mühlhäuser M., Schnell M., Peyerimhoff S. D.: *Mol. Phys.* **2002**, *100*, 509.
12. Schnell M., Mühlhäuser M., Peyerimhoff S. D.: *Chem. Phys. Lett.* **2001**, *344*, 519.
13. Schnell M., Mühlhäuser M., Peyerimhoff S. D.: *J. Mol. Spectrosc.* **2002**, *214*, 124.
14. Mühlhäuser M., Schnell M., Peyerimhoff S. D.: *Mol. Phys.* **2002**, *100*, 2719.
15. Mühlhäuser M., Schnell M., Peyerimhoff S. D.: *Photochem. Photobiol.* **2002**, *76*, 176.
16. Frisch M. J., Trucks G. W., Schlegel H. B., Gill P. M. W., Johnson B. G., Robb M. A., Cheeseman J. R., Keith T. A., Peterson G. A., Motgomery J. A., Raghavachari K., Al-Laham M. A., Zakrewski V. G., Ortiz J. V., Foresman J. B., Cioslowski J., Stefanov B. B., Nanayakkara A., Challacombe M., Peng C. Y., Ayala P. Y., Chen W., Wong M. W., Andres J. L., Replogle E. S., Matrin R. L., Fox D. J., Binkley J. S., Defrees D. J., Baker J., Stewart J. P., Head-Gordon M., Gonzales C., Pople J. A.: *GAUSSIAN 98*. Gaussian Inc., Pittsburgh (PA) 1999.
17. Poirierer R., Kari R., Csizmadia I. (Eds): *Handbook of Gaussian Basis Sets*, p. 225 (No. 6.59.4). Elsevier, Amsterdam 1985.
18. Hanrath M., Engels B.: *Chem. Phys.* **1997**, *225*, 197.
19. Buenker R. J., Peyerimhoff S. D.: *Theor. Chim. Acta* **1974**, *35*, 33.
20. Buenker R. J., Peyerimhoff S. D.: *Theor. Chim. Acta* **1975**, *39*, 217.
21. Herzberg G.: *Molecular Spectra and Molecular Structure*, Vol. II, 1st ed. Van Nostrand Reinhold Company, New York 1966.
22. Barnes R. J., Lock M., Coleman J., Sinha A.: *J. Phys. Chem. A* **1996**, *100*, 453.
23. Francisco J. S., Hand M. R., Williams I. H.: *J. Phys. Chem. A* **1996**, *100*, 9250.